LIQUID CRYSTALS, 2002, VOL. 29, NO. 11, 1477–1482

Taylor & Francis
Taylor & Francis Group

Synthesis and study of *N*,*N*-disubstituted 4-aminophenylazobenzaldehydes

LONG-LI LAI*, YU-JEN LIN, CHIA-HUSAN HO, ESHIN WANG
Department of Applied Chemistry, National Chi Nan University, Puli, Taiwan 545, ROC

YI-HUNG LIU, YU WANG
Instrumentation Center and Department of Chemistry, National Taiwan University, Taipei, Taiwan 106, ROC

YANG-CHU LIN and KUNG-LUNG CHENG
Union Chemical Laboratory, Industrial Research Institute Hsinchu, Taiwan 300, ROC

(*Received 8 March 2002; accepted 15 May 2002*)

A series of *N*,*N*-disubstituted 4-aminophenylazobenzaldehydes (azo dyes) were synthesized by the reaction of phenylpiperazine derivatives with 4-formylbenzenediazonium tetrafluoroborate. The salt was easily prepared by reacting poly(aminobenzaldehyde) with sodium nitrite in the presence of tetrafluoroboric acid. A representative sample was studied by crystallography, and the charge distribution of the molecule was calculated with the aim of understanding the form of molecular stacking on the basis of crystal data. The mesogenic behaviour of the azo dyes was also studied.

1. Introduction

Azo dye molecules have recently attracted much attention in both academic and application areas [1, 2]. For example, a dichroic dye is dissolved in a liquid crystal to give better reflectance of the polarizer [3]. Furthermore, azo dyes have a useful dichroic ratio and are suitable materials for low power consumption reflective liquid crystal devices. The three-layered guest–host systems of dichroic dye with subtractive colour mixing of yellow, magenta, and cyan are expected to be used for the development of full-colour reflective displays [4]. Previously, we have successfully synthesized several azo dye materials with the general formula **1** [5] (see the scheme), which all show smectic phases. However, nematic liquid crystals are more valuable in practical uses, as they possess lower viscosity and faster response under applied electrical switching. Therefore we attempted to synthesize a series of novel nematic azo dyes containing a CHO functionality. Such a material is useful for the further synthesis of chiral derivatives [6] which are important in developing ferroelectric and anti-ferroelectric displays [7]. To understand the molecular stacking of the nematic liquid crystals, the azo dye was studied by single crystal structure determination. Based on the molecular arrangement identified from crystallography together with charge calculation by a semi-empirical method, we find that the partial charges of the polar groups are influential on molecular stacking in the solid state. We previously published preliminary results [8], and now wish to report the complete study.

*Author for correspondence; e-mail: lilai@ncnu.edu.tw

2. Experimental

Chemicals used were commercially available from ACROS. The UV-visible absorption (λ_{max}) of compound **4b** was recorded using a HP 8453 UV-vis spectrometer, and the thermal stability was characterized by thermogravimetric analysis (Perkin-Elmer TGA 7). The mesogenic behaviour and phase transitions were characterized by polarizing optical microscopy (POM) and differential scanning calorimetry (Perkin-Elmer DSC 6). Powder X-ray diffraction (XRD) patterns were obtained with a Siemens D-5000 X-ray diffractometer equipped with a TTK 450 temperature controller and Cu radiation with $\lambda = 1.5406$ Å. Semi-empirical calculations are carried out using the CAChe program, which was provided by Fujitsu (version 3.2). The conformation of molecule **4b** was built on the basis of crystal data and then optimized by a PM3 model.

Liquid Crystals ISSN 0267-8292 print/ISSN 1366-5855 online © 2002 Taylor & Francis Ltd
http://www.tandf.co.uk/journals
DOI: 10.1080/0267829021000017708

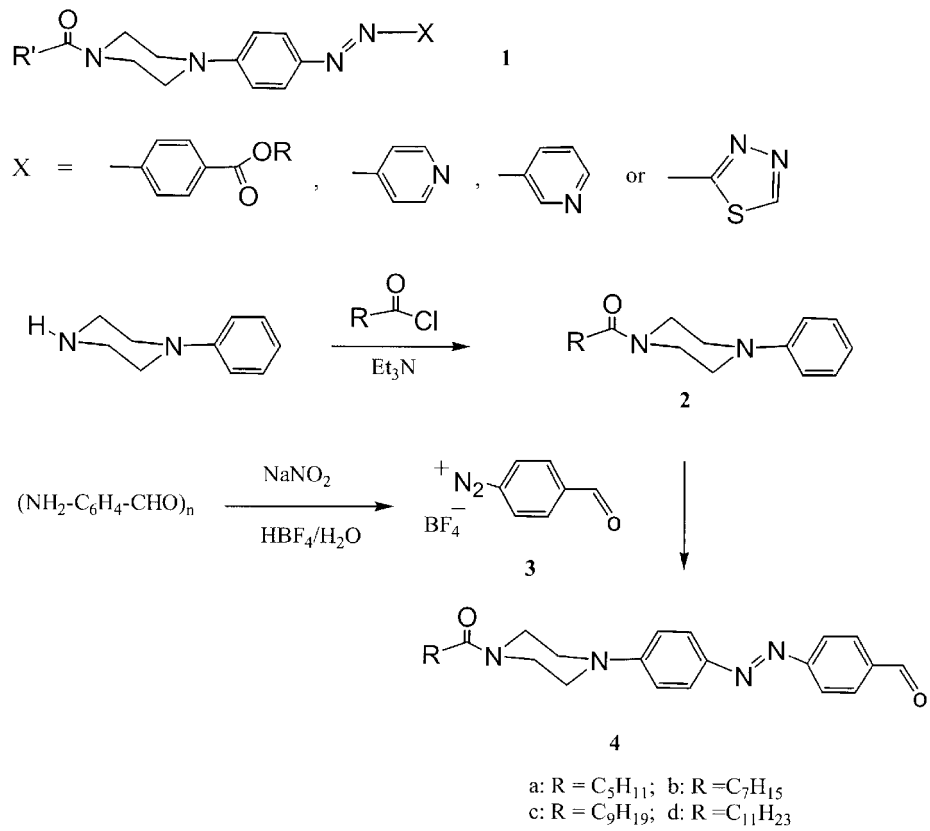

Scheme.

2.1. *Synthesis of compounds* ***4a–4d***

Poly(aminobenzaldehyde) (1.21 g, 10 mmol) was added to HBF_4 (50 wt % in water; 8 ml), and then diluted with hot water (about 90°C; 7 ml). $NaNO_2$ (1.03 g, 15 mmol) was gradually added at 0°C and the solution was held in the refrigerator overnight. Diazonium salt **3**, which had precipitated, was filtered off, washed with dry ether and dried; it was isolated in quantitative yield. The phenylpiperazine derivative **2a** (2 mmol) was added to salt **3** (2.4 mmol) in acetic acid (10 ml), and the solution stirred for 2 h at room temperature. H_2O (100 ml) was added and the mixture was extracted with CH_2Cl_2 (100 ml × 2). The combined extracts were dried over sodium sulfate and solvent was removed under reduced pressure. The residue was chromatographed on silica to give the desired azo dye **4a**, which was characterized by IR (cm^{-1}; Bio-Rad; Digilab ITS-60), ^1H NMR (Bruker 200 FT NMR spectrometer), and high resolution mass spectra (VG70-250; EI, 70 ev). Compounds **4b–4d** were prepared and characterized similarly.

4a. Yield: 30.7% (0.241 g). IR: 2954, 2852, 2718, 1698, 1635, 1598, 1513, 1456, 1429, 1391, 1371. ^1H NMR ($CDCl_3$): 0.89 (t, 3H, $J = 6.2$ Hz, CH_3), 1.29–1.36 (m, 4H, $2CH_2$), 1.57–1.66 (m, 2H, CH_2), 2.36 (t, 2H, $J = 8.0$ Hz, CH_2), 3.40 (br. s, 4H, $2CH_2$), 3.66 (br. s, 2H, CH_2), 3.80 (br. s, 2H, CH_2), 6.96 (AA′BB′, 2H, $J = 8.8$ Hz, 2Ar–H), 7.92 (AA′BB′, 2H, $J = 8.8$ Hz, 2Ar–H), 7.98 (br. s, 4H, 4Ar–H), 10.06 (s, 1H, CHO). HRMS for $C_{23}H_{28}N_4O_2$: 392.2212; found: 392.2209.

4b. Yield: 40.8% (0.342 g). IR: 2948, 2919, 2847, 2731, 1694, 1643, 1595, 1561, 1542, 1509, 1457, 1428, 1391, 1370. ^1H NMR ($CDCl_3$): 0.85 (t, 3H, $J = 6.6$ Hz, CH_3), 1.29–1.36 (m, 8H, $4CH_2$), 1.57–1.66 (m, 2H, CH_2), 2.33 (t, 2H, $J = 7.8$ Hz, CH_2), 3.40 (br. s, 4H, $2CH_2$), 3.66 (br. s, 2H, CH_2), 3.80 (br. s, 2H, CH_2), 6.95 (AA′BB′, 2H, $J = 8.8$ Hz, 2Ar–H), 7.92 (AA′BB′, 2H, $J = 8.8$ Hz, 2Ar–H), 7.97 (br. s, 4H, 4Ar–H), 10.05 (s, 1H, CHO). HRMS for $C_{25}H_{32}N_4O_2$: 420.2525; found: 420.2526.

4c. Yield: 32.7% (0.293 g). IR: 2919, 2848, 2727, 1698, 1645, 1596, 1567, 1506, 1438, 1377. ^1H NMR ($CDCl_3$): 0.89 (t, 3H, $J = 6.6$ Hz, CH_3), 1.29–1.36 (m, 12H, $6CH_2$), 1.57–1.66 (m, 2H, CH_2), 2.36 (t, 2H, $J = 7.8$ Hz, CH_2), 3.40 (br. s, 4H, $2CH_2$), 3.66 (br. s, 2H, CH_2), 3.80 (br. s, 2H, CH_2), 6.96 (AA′BB′, 2H, $J = 8.8$ Hz, 2Ar–H), 7.92 (AA′BB′, 2H, $J = 8.8$ Hz, 2Ar–H), 7.98 (br. s, 4H, 4Ar–H), 10.06 (s, 1H, CHO). HRMS for $C_{27}H_{36}N_4O_2$: 448.2838; found: 488.2837.

4d. Yield: 32.7% (0.306 g). IR: 2919, 2851, 2727, 1693, 1641, 1598, 1507, 1466, 1437. ^1H NMR ($CDCl_3$): 0.89 (t, 3H, $J = 6.6$ Hz, CH_3), 1.29–1.36 (m, 16H, $8CH_2$), 1.57–1.66 (m, 2H, CH_2), 2.36 (t, 2H, $J = 7.8$ Hz, CH_2), 3.40 (br. s, 4H, $2CH_2$), 3.66 (br. s, 2H, CH_2), 3.80

(br. s, 2H, CH_2), 6.96 (AA′BB′, 2H, $J = 8.8$ Hz, 2Ar–H), 7.92 (AA′BB′, 2H, $J = 8.8$ Hz, 2Ar–H), 7.98 (br. s, 4H, 4Ar–H), 10.06 (s, 1H, CHO). HRMS for $C_{29}H_{40}N_4O_2$: 476.3151; found: 476.3152.

2.2. *X-ray crystallography analysis*

Crystals of compound **4b** were grown from dichloromethane/hexane (1/1) at room temperature. A single crystal of suitable quality was mounted on a glass fibre and used for measurement of precise cell constants and intensity data collection. Diffraction measurement was made on a Siemens SMART 1K CCD diffractometer with graphite-monochromated Mo-Kα radiation ($\lambda = 0.71073$ Å), operated at 150(2) K over the θ range of 1.54–23.26°. No significant decay was observed during the data collection. 2269 reflections were observed with $I \geqslant 2\sigma(I)$ among the 3188 unique reflections, and 2987 reflections were used in the refinement. Data were processed on a PC using SHELXTL software package [9]. The structure of **4b** was solved using the direct methods and refined by full-matrix least square on F^2 value. All non-hydrogen atoms were refined anisotropically. The hydrogen atoms were fixed at calculated positions and refined using a riding model. The final indices were $R1 = 0.0441$, $wR2 = 0.0901$ with goodness-of-fit on $F^2 = 1.000$. The crystal data are summarized in table 1; selected bond lengths and angles are given in table 2.

3. Results and discussion

3.1. *Synthesis and physical study*

Compounds **2a–2d** were prepared from the reaction of phenylpiperazine with appropriate alkanoyl chlorides in dichloromethane in the presence of triethylamine; they were obtained in almost quantitative yields. The *N*,*N*-disubstituted 4-aminophenylazo benzaldehydes **4a–4d** were synthesized by the reaction of compounds **2a–2d**, respectively, with diazonium salt. Although the corresponding salt can be synthesized from freshly prepared 4-aminobenzaldehyde [10], the storage of the salt precursor is a problem: it gradually loses water during storage. We thus simplified the salt preparation by hydrolysing commercially available poly(4-aminobenzaldehyde) in hot tetrafluoroboric acid solution and then allowing the resulting ammonium benzaldehyde to react with 1.5 equivalents of $NaNO_2$ at 0°C (see the scheme) [8]. Compound **4b** representing this series of azo dyes was investigated by UV-visible absorption spectroscopy and found to have a visible absorption (λ_{max}) at 428 nm in dichloromethane. When compared with the absorption (λ_{max}) of compound **1** (X = benzoate or pyridyl), a 16 nm red-shift occurs. In particularly, compound **4b** is reasonably stable, and only starts to decompose at about 270°C during thermogrammetric analysis.

The nematic phases of compounds **4a–4c** on heating and cooling (table 3), were characterized by their schlieren texture by POM; compound **4b** was further characterized by powder XRD. The nematic ranges for compounds **4a–4c** decrease with increasing the length of alkyl chain. The mesogenic ranges on cooling are about 60, 51 and 27°C for compounds **4a**, **4b** and **4c**, respectively. As there is no layer structure in the nematic range for liquid crystals, no small angle reflection was observed for compound **4b** in XRD. However compound **4d** shows a SmC phase during heating and cooling; this was characterized by a broken focal-conic texture coexisting with a schlieren texture, together with low viscosity under POM. The SmC phase of compound **4d** was also characterized by powder XRD; layer distances were 40.44, 40.08 and 40.05 Å at 160, 140 and 120°C, respectively.

Table 1. Crystallographic data for compound **4b**.

Formula	$C_{25}H_{32}N_4O_2$
Formula weight	420.55
Space group	$P2_12_12_1$
a/Å	7.4709(7)
b/Å	11.2442(10)
c/Å	26.389(3)
$\alpha = \beta = \gamma$	90°
v/Å^3	2216.8(4)
Z	4
D_c/g cm^{-3}	1.260
μ/cm^{-1}	0.081
$2\theta_{max}$/deg	46.52
Reflections measured	8787
Reflections used (R_{int})	3188(0.0486)
Final $R[I > 2\sigma(I)]$	$R1^a = 0.0441$, $wR2^b = 0.0901$
R (all data)	$R1 = 0.0782$, $wR2 = 0.1162$
Goodness-of-fit on F^2	1.000

[a] $R1 = \Sigma|F_c|/\Sigma|F_0|$

[b] $wR2 = [\Sigma w[(F_0^2 - F_c^2)^2]/\Sigma w(F_0^2)^2]]^{1/2}$: $w = 1/[\sigma^2(F_0^2) + (0.08P)^2]$, where $P = [\max(F_0^2, 0) + 2F_c^2)/3$.

Table 2. Selected bond lengths (Å) and angles (°) for compound **4b**.

Bond lengths			
O1–C1	1.235(4)	O1–C25	1.211(4)
N1–C1	1.356(4)	N1–C12	1.458(4)
N1–C9	1.463(4)	N2–C13	1.395(4)
N2–C11	1.466(4)	N2–C10	1.470(4)
N3–N4	1.271(4)	N3–C16	1.409(4)
N4–C19	1.432(4)		
Bond angles			
C1–N2–C12	125.0(3)	C1–N1–C9	120.9(3)
C12–N1–C9	111.3(3)	C13–N2–C11	118.4(3)
C13–N2–C10	117.9(3)	C11–N2–C10	113.1(3)
N4–N3–C16	113.8(3)	N3–N4–C19	113.3(2)
O1–C1–N1	121.3(3)	O1–C1–C2	121.4(3)
N1–C1–N1	117.3(3)	C17–C16–N3	125.0(3)
C15–C16–N3	116.6(3)	C20–C19–N4	124.5(3)
C24–C19–N4	114.8(3)		

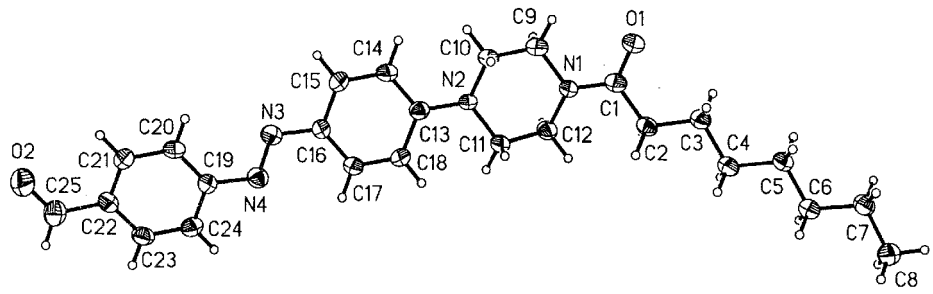

Figure 1. The structure of compound **4b**.

Table 3. Phase transition temperatures (°C) and corresponding enthalpies (kJ mol^{-1}), in parentheses, of compounds **4a**–**4d**. The phase transition temperatures and corresponding enthalpies of compounds **4a**–**4d** were determined by 2nd DSC scans at a heating and cooling rate of 10° min^{-1} between 50 and 200°C. Abbreviations: Cr = crystalline, N = nematic, SmC = smectic C phase, I = isotropic liquid.

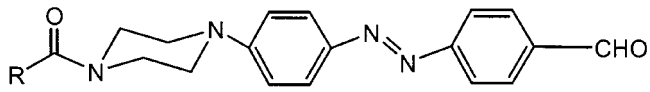

4

4a, $R = C_5H_{11}$	Cr	144.3(19.9) / 117.7(20.8)	N	177.4(0.2) / 177.3(0.2)	I
4b, $R = C_7H_{13}$	Cr	125.4(19.4) / 107.0(19.2)	N	158.7(0.3) / 158.3(0.3)	I
4c, $R = C_9H_{19}$	Cr	149.3(21.4) / 137.0(20.9)	N	164.7(0.3) / 164.3(0.3)	I
4d, $R = C_{11}H_{23}$	Cr	121.5(16.0) / 104.3(16.3)	SmC	162.7(1.5) / 162.6(1.6)	I

3.2. *Structure determination and molecular modelling*

Compound **4b**, representative of this series of molecules, was studied by single crystal structure determination (figure 1). The dihedral angles between the plane containing C19–N3–N4–C16 and two benzene rings (C13 ~ C18 and C19 ~ C24) are 2.96° and 10.45°, respectively. The N3–N4 bond (1.271 Å) is slightly longer than that of a typical *trans* N=N bond (1.222 Å). Consistently, the N2–C13 bond (1.395 Å) is rather shorter than that of a typical N_{sp3}–C_{sp2} bond (1.416 Å) [11]. This indicates that the donation of electron density from atom N2 to the N=N group is significant. The N3–C16 bond, to some extent, thus possesses the greater π-electron character. However the influence of the electron withdrawing C=O group is reductive when compared with that of the N2 atom, and the N4–C19 bond (1.432 Å) possesses less π-electron character. Consequently, the dihedral angle between the plane containing C19–N3–N4–C16 and the C13 ~ C18 ring (2.96°) is smaller than that between the plane containing C19–N3–N4–C16 and the C19 ~ C24 ring (10.45°), because of the difference in π-electron conjugation.

The representative molecular stacking of compound **4b** in the solid state, obtained from single crystal structure determination, is shown in figure 2. Molecules a, b and e are approximately parallel to each other and arranged face-to-face as a vertical layer. Molecule b is, however, packed oppositely between molecules a and e. The distances N1a-C25b and O1a-C25b are 3.60 and 3.83 Å, respectively. Molecules e and f are in horizontal contact by a side-to-side arrangement in which the distances O2e-C12f and O2e-C2f are 3.55 and 3.87 Å, respectively. The distances O2e ... H (at C12f) and O2E ... H (at C2f) are 2.71 and 2.99 Å, respectively, which are approximately equal to the sum of the van der Waals radii of H and O (Bondi radii: H 1.20, O 1.52) [12*a*]. The H-bond interaction arising thereof should be influential in the horizontal molecular stacking arrangement [12*b*].

To understand how the functional groups influence the molecular stacking of compound **4b**, we further calculated the partial charges of molecule **4b** by the CAChe program (version 3.2). The conformation of molecule **4b** was built on the basis of crystal data and then optimized by the PM3 model. For simplicity, only part of the calculated results is shown in figure 3. The partial charges of C-atoms of the aldehyde and amido functionality are the most positive (0.33 and 0.26, respectively). The partial charges of the corresponding O-atoms are the most negative (−0.33 and −0.37, respectively). Therefore, we conclude that the interaction between molecules is stronger in the vicinity of the

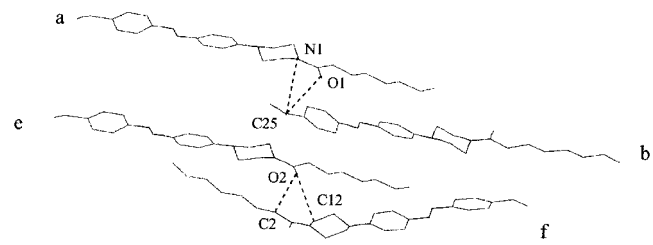

Figure 2. The representative molecular stacking of compound **4b**.

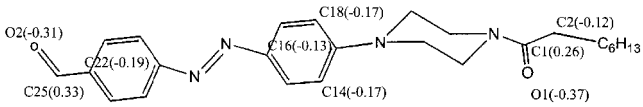

Figure 3. Part of the partial charges (non-H atoms) of molecule **4b**, obtained by PM3 model; the partial charges of other atoms (not indicated) are equal to or less than $|-0.1|$.

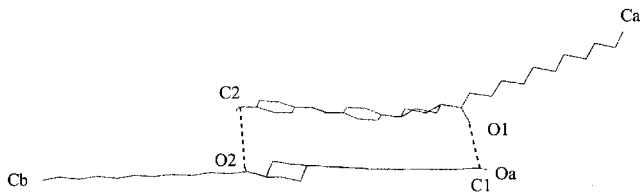

Figure 4. A possible arrangement of **4d** dimers for the formation of the SmC phase during the thermal process. The heats of formation for two molecules were calculated to be 50.11 and 50.29 kcal mol^{-1}. The heat of formation of the dimers was calculated to be 89.86, and the energy of the system is thus lowered by 10.54 kcal mol^{-1}. The distance Ca-Cb is calculated to be 41.94 Å. The calculation was carried out by augmented MM3 parameters.

aldehyde and amido moieties in the solid state, which is consistent with the crystallographic results as discussed previously.

It is noteworthy that the alkyl chain length influences the mesogenic behaviour of this series of azo dyes. As compounds **4a**–**4d** consist of the same rigid core with a variable length alkyl chain, it is reasonable to assume that they should have similar conformations in the gas phase. We therefore calculated the conformation of molecule **4d** on the basis of crystallographic data of compound **4b**. Accordingly, molecule **4d** was optimized using the PM3 model. After optimization, the length of the extended molecule **4d** was calculated to be 29.68 Å, which is much shorter than its d-spacing in the SmC phase. Thus, the latter should be measured from the dimer unit of **4d**. To work out the possible arrangement of a dimer of **4d**, we calculated the charge distribution of molecule **4d**; a similar result to that for molecule **4b** was obtained. This suggested that the aldehyde and amido moieties are still influential in the molecular stacking. However the powder XRD patterns for compounds **4b** and **4d** are different at room temperature(†), which indicates that the crystal packing for compounds **4b** and **4d** may be different. Therefore, a possible arrangement for the **4d** dimer was proposed as shown in figure 4, where the distances C1-O1 and C2-O2 are 3.31 and 4.27 Å, respectively. The distance Ca-Cb was calculated to be 41.94 Å, which is slightly longer than the d-spacing (40.05 Å at 120°) obtained from the powder XRD study. As there is a tilt angle between the molecular and Z axes, the fully extended dimer is longer than the d-spacing (Z component of an extended molecular length) in the SmC range.

† The wide angle (15–25°) construction reflection for compound **4b** was found at distances of 5.42, 5.11, 4.94, 4.32, 4.15, 3.74 and 3.68 Å. The wide angle (15–25°) construction reflection for compound **4d** was found at distances of 5.21, 4.34 and 3.72 Å.

4. Conclusion

This work presents a convenient synthesis of nematic azo dye liquid crystals containing a CHO functional group; they are found to be reasonably thermo-stable. The results of crystallographic study provide details of the crystal packing in the solid state and the correlated positions of the molecules. It is noteworthy that the successful strategy of combining crystallography and simple molecular modelling, for a detailed study of the molecular interaction, provides useful experience in the liquid crystal field.

We thank the National Chi Nan University and the National Science Council (NSC 90-2113-M-260-002) for financial support. The National Center of High-Performing Computing and the Institute of Chemistry, Academia Sinica, are also highly appreciated for providing the Beilstein database system and the XRD apparatus, respectively.

References

[1] (*a*) Feringa, B. L., Van Delden, R. A., Koumura, N., and Geertsema, E. M., 2000, *Chem. Rev.*, **100,** 1789; (*b*) Kawata, S., and Kawata, Y., 2000, *Chem. Rev.*, **100,** 1777; (*c*) Delaire, J. A., and Nakatani, K., 2000, *Chem. Rev.*, **100,** 1817; (*d*) Ichimura, K., 2000, *Chem. Rev.*, **100,** 1847; (*e*) Tamai, N., and Miyasaka, H., 2000, *Chem. Rev.*, **100,** 1875; (*f*) Shirota, K., and Yamaguchi, I., 2000, *Liq. Cryst.*, **27,** 555.

[2] (*a*) Ruslim, C., and Ichimura, K., 1998, *Chem. Lett.*, 789; (*b*) Kozlovsky, M. V., Sibaev, V. P., Stakhanov, A. I., Weyrauch, T., and Haase, W., 1998, *Liq. Cryst.*, **24,** 759; (*c*) Shivaev, V. P., Kostomin, S. G., and Ivanov, S. A., 1996, *Polymer as Electrooptical and Photooptical Active Media*, edited by V. P. Shibaev (Berlin: Springer), pp. 37–110; (*d*) Ikeda, T., and Tsutsumi, O., 1995, *Science*, **268,** 1873; (*e*) Anderle, K., and Wendorff, J., 1994, *Mol. Cryst. liq. Cryst.*, **243,** 51; (*f*) Hermann, D. S., Rudquist, P., Ichimura, K., Kudo, K., Komitov, L., and Lagerwall, S. T., 1997, *Phys. Rev. E*, **55,** 2857; (*g*) Sasaki, T., Ikeda, T., and Ichimura, K., 1994, *J. Am. chem. Soc.*, **116,** 625.

[3] (*a*) Broer, D. J., and Lub, J., 1996, US patent 55 06 704; (*b*) Berke, C. M., 1982, US patent 44 40 541.

[4] (*a*) Sunohara, K., Naito, K., Tanaka, M., Naikai, Y., Kamiura, N., and Taira, K., 1996, *SID'96 Dig.*, p. 103; (*b*) Taira, K., Iwanaga, H., Hotta, A., Nakai, Y., Ohtake, T., and Sunohara, K., 1996, *AM-LCD'96*, p. 333; (*c*) Tanaka, M., 1997, *FPD Intelligence*, **4,** 70; (*d*) Bauman, D., 1988, *Mol. Cryst. liq. Cryst.*, **159,** 197.

[5] (*a*) Lai, L. L., and Lin, H.-C., 2000, *Liq. Cryst.*, **27,** 707; (*b*) Lai, L. L., Lee, L. J., Lee, G. H., Wang, Y., Lu, K. L., and Lee, S. J., 2001, *Liq. Cryst.*, **28,** 1513; (*c*) Lai, L. L., Wang, E., Lee, L. J., Chen, J. J., and Yang, D. W., 2001, *Liq. Cryst.*, **28,** 157; (*d*) Lai, L. L., Lee, L. J., Wang, E., and Su, F. Y., 2001, *Liq. Cryst.*, **28,** 381; (*e*) Lai, L. L., and Wang, E., 2001, *Helv. Chim. Acta*, **84,** 3581.

[6] Soai, K., and Niwa, S., 1998, *Chem. Rev.*, **92,** 833.

[7] (*a*) Rudquist, P., Lagerwall, J. P. F., Buivydas, M., Gouda, F., Lagerwall, S. T., Clark, N. A., Maclennan, J. E., Shiao, R., Coleman, D. A., Bardon, S., Bellini, T., Link, D. R., Natale, G., Glaser, M. A., Walba, D. M., Wand, M. D., and Chen, X. H., 1999, *J. mater. Chem.*, **9,** 1257; (*b*) Beccherelli, R., and Elston, S. J., 1998, *Liq. Cryst.*, **25,** 573; (*c*) Chen, Y., and Wu, W. J., 1998, *Liq. Cryst.*, **25,** 309.

[8] Lai, L. L., Ho, C. H., Lin, Y. J., Wang, E., Liu, Y. H., Wang, Y., Lin, Y. C., and Cheng, K. L., 2002, *Helv. Chim. Acta.*, **85,** 108.

[9] Sheldrick, G. M., 1944, *SHELXTL* version 5.03, Siemens Analytical X-ray Instruments Inc. Madison, Wisconsin.

[10] (*a*) Yasuhara, A., Kasano, A., and Sakamoto, T., 1999, *J. org. Chem.*, **64,** 2301; (*b*) Fritz-Langhals, E., and Kunath, B., 1998, *Tetrahedron Lett.*, **39,** 5955.

[11] Allen, F. A., Kennard, O., Watson, D. G., Brammer, L., Orpen, A. G., and Taylor, R., 1987, *J. chem. Soc. Perkin Trans II*, S1-S19.

[12] (*a*) Bondi, A., 1964, *J. phys. Chem.*, **68,** 441; (*b*) Allen, R. H., Lommerse, J. P. M., Hoy, V. J., Howard, J. A. K., and Desiraju, G. R., 1996, *Acta Cryst.*, **B52,** 734.